

Assessment of spatial distribution of soil heavy metals using ANN-GA, MSLR and satellite imagery

Arman Naderi · Mohammad Amir Delavar · Babak Kaboudin ·
Mohammad Sadegh Askari

Received: 22 August 2016 / Accepted: 6 February 2017 / Published online: 13 April 2017
© Springer International Publishing Switzerland 2017

Abstract This study aims to assess and compare heavy metal distribution models developed using stepwise multiple linear regression (MSLR) and neural network-genetic algorithm model (ANN-GA) based on satellite imagery. The source identification of heavy metals was also explored using local Moran index. Soil samples ($n = 300$) were collected based on a grid and pH, organic matter, clay, iron oxide contents cadmium (Cd), lead (Pb) and zinc (Zn) concentrations were determined for each sample. Visible/near-infrared reflectance (VNIR) within the electromagnetic ranges of satellite imagery was applied to estimate heavy metal concentrations in the soil using MSLR and ANN-GA models. The models were evaluated and ANN-GA model demonstrated higher accuracy, and the autocorrelation results showed higher significant clusters of heavy metals around the industrial zone. The higher concentration of Cd, Pb and Zn was noted under industrial lands and irrigation farming in comparison to barren and dryland farming. Accumulation of industrial wastes in roads and streams was identified as

main sources of pollution, and the concentration of soil heavy metals was reduced by increasing the distance from these sources. In comparison to MSLR, ANN-GA provided a more accurate indirect assessment of heavy metal concentrations in highly polluted soils. The clustering analysis provided reliable information about the spatial distribution of soil heavy metals and their sources.

Keywords Genetic algorithm · Hybrid model · Local Moran · Neural network

Introduction

Environmental contaminations of heavy metals due to point and non-point sources have been an important issue regarding human and animal's health (Kabata-Pendias 2010). Several factors such as agricultural activities (Liu et al. 2013), land use type (Liu et al. 2006a) and traffic (Yan et al. 2013a,b Werkenthin et al. 2014) can affect the spatial and temporal patterns of soil heavy metals. Heavy metals are metals with an atomic mass of over 55.8 g mol^{-1} or a density of over 5 g cm^{-3} (Mance and Worsfold 1988). The high resistance of heavy metals against biodegradation alongside their low mobility in soil and their tendency to be absorbed by plants are among the properties which have caused these metals to be considered as the most hazardous soil contaminant (Fu and Wang 2011). Arsenic, mercury, zinc, lead, cadmium, chromium, copper, manganese, nickel and vanadium are among the most important harmful rare elements found in the biosphere (Kabata-Pendias 2010). Sphalerite is the

The original version of this article was revised: The first and fourth authors publication names should have been Arman Naderi and Mohammad Sadegh Askari instead of Arman Nadari and Mohammad Sadegh Askari.

A. Naderi · M. A. Delavar (✉) · M. S. Askari
Department of Soil Science, Faculty of Agriculture, University of
Zanjan, Zanjan, Iran
e-mail: amir-delavar@znu.ac.ir

B. Kaboudin
Department of Chemistry, Institute for Advanced Studies in Basic
Sciences, Gavazang, Zanjan, Iran

main ore of zinc which is found in three forms including sphalerite, wurtzite and matraite (Cook et al. 2009). The level of zinc present in the lithosphere was estimated to be 80 mg kg^{-1} and the natural value of zinc in soils was stated as $10\text{--}300 \text{ mg kg}^{-1}$ (Kabata-Pendias 2010). The concentration of lead in soils is between 1 and 200 mg kg^{-1} , on average is 15 mg kg^{-1} and its critical limit is 50 mg kg^{-1} (Zimdahl and Skogerboe 1977). Cadmium and lead are two metals resulting from combustion activities and transportation and are linked to zinc resulting from abrasion of tires. Cadmium and lead are considered to be the most mobile and least mobile elements in soil with typical values of 0.06–1.1 and 2–300 mg kg^{-1} , respectively (Kabata-Pendias 2010). The maximum allowable limit for cadmium in agricultural products has been reported to be 0.1 mg kg^{-1} and in non-agricultural crop, this value should not exceed the allowable limit (Asami 1984).

At high concentrations, heavy metals are highly dynamic (Guala et al. 2010) and can easily emerge on plant components (Meindl et al. 2014) and animal products (Wang et al. 2013; Shahbazi et al. 2016) via soil contamination. Consequently, there is need to monitor and evaluate the amount and distribution of soil heavy metals (Choe et al. 2008). Developing a time and cost-effective method that can efficiently assess the concentration and distribution of heavy metals is of particular interest to land managers and scientists (Askari et al. 2015).

Remote sensing, VNIR spectroscopy have been used as rapid and practical approaches for determining the distribution of heavy metals (Hong-Yan et al. 2009). Many researches have confirmed that high concentrations of heavy metals represent electromagnetic spectrum features within the VNIR region (Shi et al. 2014) and these spectral characteristics can be employed to estimate heavy metal concentrations (Choe et al. 2008). Fe oxide, clay and organic matter contents of the soil affect spectral intensity (Dube et al. 2001; Shi et al. 2014; Wang et al. 2014), which can have an impact on the predictability of soil properties. Asmaryan et al. (2014) suggested the utilization of VNIR ranges (400–2500 nm) of electromagnetic spectrum for the detection of Pb, Cr, V, Ti, Cu, Zn and Mn in the soil. They demonstrated the positive relationships between the digital values of a satellite image within 400–510 nm and Pb, Zn and Cr between the ranges of 580–625, 630–690, 770–895 nm and other heavy metals. The linear relationships provided for Zn, Cr and Pb demonstrated an R^2 of 0.95, 0.85 and 0.83, respectively. Xia et al. (2006) found similar results and reported that Cd

concentration prediction was related to the electromagnetic features of Fe oxides and clay minerals within the range of 450–720 nm. Gannouni et al. (2012) reported that the spectral features of Fe-related and clay minerals were indirectly associated with the geochemical analysis of heavy metals. They suggested that the predictions of Mn, Pb and Zn concentrations using PLSR provide the best results within the range of 400–2500 nm.

Linking heavy metal contents to spectral absorptions using MSLR and other linear regressions has been utilized by several researchers, leading to the prediction of models with high accuracy (Choe et al. 2008; Moros et al. 2009; Gill and Tuteja 2011; Chen et al. 2012; Wang et al. 2014; Song et al. 2015). Kemper and Sommer (2002) applied stepwise multiple linear regression (MSLR) for predicting As, Cd, Cu, Fe, Hg, Pb, Sb and Zn distribution and obtained the accurate models for most of the elements.

Artificial neural network (ANN) models are used for the monitoring of heavy metals (Boszke and Astel 2009), and also, some researchers have tried to establish mathematical relationship between land characteristics and satellite data employing smart methods such as ANN (Şenkal 2010; Thenkabail et al. 2011) and genetic algorithm (GA) (Wu et al. 2015; Miao et al. 2015; Lasaponara et al. 2016). Among them, the ANN-GA hybrid model has been widely used to study the non-linear relationship between earthy measurements and satellite data. It has been reported that the model developed based on ANN-GA is more accurate than the linear models (Xiao et al. 2014; Miao et al. 2015). Generally, in monitoring process, genetic algorithm is employed for optimizations of model parameters (Icaga 2005; Chang et al. 2006). Zhou et al. (2015) applied the principal component analysis, ANN, and ANN-GA hybrid approaches to model the distribution of soil heavy metals. They concluded that the most accurate models were obtained by ANN-GA.

Identifying the source of heavy metal contamination is as important as monitoring their spatial distribution. Different tools such as clustering analysis (Templ et al. 2008) and fuzzy clustering (Pourjabbar et al. 2014) can be employed to identify the source of heavy metals. The spatial autocorrelation technique has also been reported as an appropriate approach for the source identification (Liu et al. 2006b; Zhang et al. 2008). Getis G index (Getis and Ord 1992) and spatial statistics (Ishioka et al. 2007) can also be used to identify and measure hotspots for spatial statistics of heavy metals. Moreover, local Moran's index was reported as a practical method for identifying hotspots based on neighborly relations as

well as to estimate the levels of spatial correlation among studied variables (Overmars et al. 2003; Fu et al. 2011).

Owing to the existence of several rich mines of lead and zinc in Zanjan province, many factories and industrial areas are located in this part of Iran. These industrial zones have led to heavy metal pollution in many areas of this province, due to the accumulation of industrial wastes and sewages around factories. The pollution of heavy metals can easily be dispersed into the environment by factors such as wind, surface water and transportation. The polluted lands in Zanjan put human and animal health at risk and cause environmental issues. Therefore, in this study, the distributions of heavy metals along with the main natural and artificial factors affecting their distribution were explored using remote sensing imagery. The objectives were to compare the modeling of cadmium, lead and zinc distribution using AAN-GA and multiple stepwise linear regression and to cluster polluted area by local Moran index and Getis-Ord G^* statistics for source identification. Furthermore, the effects of different land uses on the concentration of elements and distribution of heavy metals around highways, main roads, railroads and streams were studied.

Materials and methods

Study area

The study was carried out in east Zanjan, Iran (36.58–36.67° N and 48.57–48.67° E, Fig. 1). According to the meteorological data of Zanjan synoptic stations, which is over a period of 39 years (1975 to 2014), the study area has four distinctive seasons with a mean annual temperature of 15.7 °C and a mean annual precipitation of 309 mm. Prevailing wind speed (east to west) is 6.4 m s⁻¹. The Tabriz-Tehran freeway (line 1 in Fig. 1) and expressway of Basij (line 2 in Fig. 1) passed through the study area.

Soil sampling and analyses

A total of 300 sites were sampled from May 19 to 29, 2014, in different land uses including industrial lands, irrigated farming, dryland farming and barren lands. Soil samples were collected in two grids at intervals of 250 m for area close to industrial and agricultural land and 500 m for bare lands, at 0–5-cm soil depths. Soil

samples were air-dried and passed through a 2-mm sieve. pH (pH meter model 215 Meter, Denver Instrument), total Fe (Mehra and Jackson 1958), organic carbon (Walky and Black 1934), sand, silt and clay contents (Gee et al. 1986) were measured for each sample. The concentrations of Cd, Pb and Zn were measured using graphite furnace atomic absorption spectrometry (Varian spectra AA-200, Analytic Jena). The instrument was calibrated by using 1000 mg titrisol standard solutions (CdCl₂ in H₂O, Pb(NO₃)₂ in H₂O and ZnCl₂ in 0.06% HCl (Merck Company)). Each sample was measured in triplicate, and the relative standard deviations (%RSD) of the heavy metal concentrations were applied to determine the measurement method precision using Eq. (1):

$$\%RSD = \text{standard deviation} / \text{mean value} \times 100 \quad (1)$$

To assess the accuracy of heavy metal measurement, the recovery test was conducted. The percentage recovery (%REC) was calculated using Eq. (2):

$$\%REC = (C_s - C) / C_{\text{add}} \times 100 \quad (2)$$

where C_s is the concentration of spiked sample (added sample + measured sample), C is the concentration of unspiked sample (measured sample) and C_{add} is the concentration of added sample.

Data analysis

Image processing was performed using Landsat ETM + imagery (ID LE07_L1TP_166035_20140527_20161115_01_T1, acquisition date May 27, 2014, path 166, row 35). The most important corrections made in this research include atmospheric correction, geometric correction, and the correlation related to noise in the image. In this research, fast line of sight atmospheric analysis of spectral hypercubes (FLAASH) algorithm was employed to correct the atmospheric effects. Using this algorithm, the values of the spectral radiation were converted to spectral reflection, and the effects associated with the changes in the lighting conditions, season, latitude, and meteorological conditions on the images were removed. In order to remove noise in the images used, minimum noise fraction transform (MNFT) algorithm was employed by ENVI software. This conversion is a linear conversion which is employed for determining the main dimension and volume of the image, separating noise from other information, and

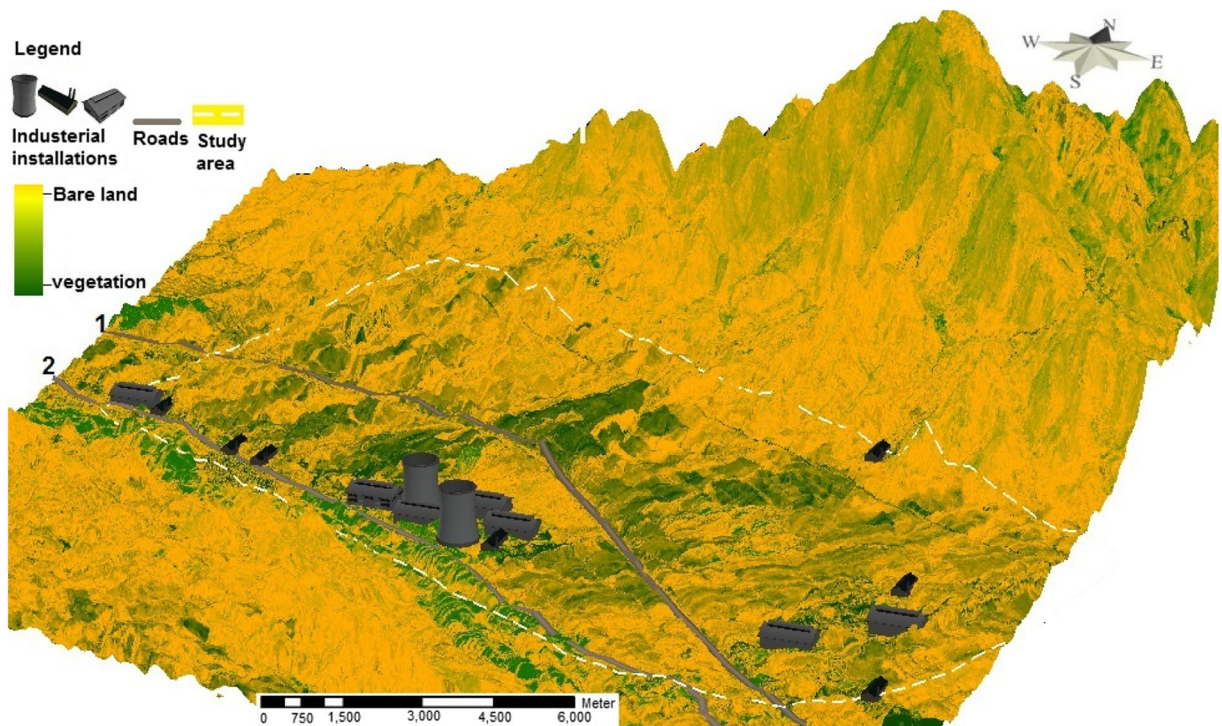


Fig. 1 a Location map of study area, industrial installations and roads including Tehran-Tabriz freeway (1) and Basij Expressway (2)

reducing the extent of process in the next stage. In the last stage, following application of all required corrections, the geometrical correction of the image was used by ground control points which were extracted from topography maps at a scale of 1:25,000 and existed throughout the

entire region sporadically. For this purpose, the geographical position of 40 points was withdrawn using global positioning system device (GPS model Garmin 41838), and the geometrical correction was performed on the image. After atmospheric and geometric corrections, the

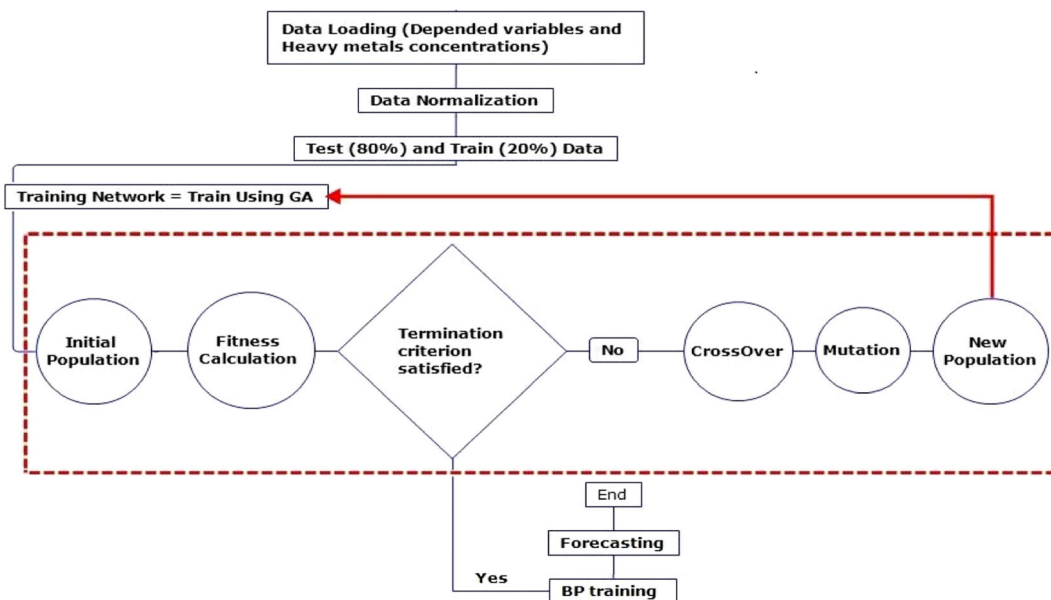


Fig. 2 A schematic representation of ANN-GA model

Table 1 Statistical description soil properties

Properties	Sample number	Min	Max	Mean	St. dv.
pH	300	6.69	8.33	7.71	2.12
OC (%)	300	0.45	1.25	0.78	0.18
Clay (%)	300	17.11	34.18	26.51	7.91
Sand (%)	300	51.22	81.61	62.64	5.55
Silt (%)	300	6.82	35.50	18.87	5.61
Fe (%)	300	0.89	1.30	0.95	0.10

mean values of digital numbers within a radius of 30 m around the sampling points were determined for each band in MATLAB (R2014a). Shapiro-Wilk test was used to assess the normality of residual.

To remove the weakest correlated variable, MSLR was applied. This technique minimizes the sum of squared deviations of the observed and predicted dependent variables via the linear transformations of the independent variables. The relationship between heavy metal concentration (as a dependent variable) and averages of pixel values and soil properties (as independent variables) were determined for each band and band ratio by applying MSLR analysis. The band ratios are considered to be absolutely useful methods for highlighting phenomena like heavy metal in multiband images (Kaiser et al. 2010; Slonecker et al. 2010).

Hybrid ANN-GA method was used for modeling by using feedforward multilayer perceptron neural networks alongside sigmoid transfer functions with the application of organic carbon, total Fe and clay contents. Moreover, Landsat bands (band 1 0.52–0.45 μm, band 2 0.60–0.52 μm, band 3 0.63–0.60 μm, band 4 0.90–0.75 μm, band 5 1.75–1.55 μm, band 6 12.50–10.40 μm, and band 7 2.35–2.09 μm) were used as an independent variable for ANN-GA and MSLR modeling.

Table 2 Statistical description of the heavy metal concentration (mg kg⁻¹) and related risk classification

Element	Sample number	Statistical analysis					Risk classification levels (DEIRI 2013)		
		Min (mg kg ⁻¹)	Max	Mean	RSD %	REC	No risk (mg kg ⁻¹)	Risk	High risk
Cd	300	0.88	17.61	1.92	0.82	86–105	0–5	5–13	>13
Pb	300	13.38	3475	354.98	2.01	91–107	0–75	75–520	>520
Zn	300	12.50	7253.6	501.10	1.01	90–112	0–360	360–6800	>6800

Table 3 Cross-validation results of ANN-GA and MSLR models for Cd, Pb and Zn (mg kg⁻¹)

Model	Cd	Pb	Zn
R ² _{tr} (ANN-GA)	0.85	0.91	0.90
R ² _{tr} (MSLR)	0.41	0.58	0.57
R ² _{ts} (ANN-GA)	0.91	0.86	0.76
R ² _{ts} (MSLR)	0.51	0.56	0.63

tr train data, *ts* test data

To adjust the weights of the neurons connected in the hybrid ANN-GA model, GA was adopted in the ANN training process to identify the best solution by mutation and crossover operators and evaluation by R² and RMSE in the output layer (Fig. 2).

A total of 240 (80%) and 60 (20%) samples were randomly allocated to the training and testing sets, respectively. The accuracy of models was assessed using predictions coefficient of determination (R²) and root mean square error (RMSE). Data analysis and processing of satellite images were performed in ENVI software, and maps were prepared using ArcGIS software version 10.2. To investigate the spatial autocorrelation analysis, the local Moran I (Anselin 1995) (Eq. (3)) and G* statistical method (Getis and Ord 1992) (Eq. (4)) were used to identify the presence of clusters:

$$I_i = x_i \sum_{j=1, j \neq i}^N w_{ij} x_j \tag{3}$$

where *I_i* is the Moran index, *N* is the number of spatial observation pixel, *x_i* is the standardized observed value of pixel *i*, *x_j* is the standardized observed value of pixel *j*, and *w_{ij}* is the the standardized spatial weighting value.

Table 4 MSLR for heavy metal concentrations and independent variables (soil properties and satellite imaginary bands)

Element	Band formulation used in the models
Cd	$-221.676 + 60.2 \text{ OC} + 0.1 \text{ clay} + 11.4 \text{ Fe} + 164.6 (\text{band } 2 / \text{band } 3) + 95.3 (\text{band } 3 / \text{band } 2) + 0.1 (\text{band } 4) - 3.7 (\text{band } 5 / \text{band } 1)$
Pb	$-180,599.0 + 45.1 \text{ OC} + 32.2 \text{ clay} + 18.7 \text{ Fe} + 156,204 (\text{band } 2 / \text{band } 3) - 53.1 (\text{band } 4) + 2615.5 (\text{band } 7 / \text{band } 1) - 20,830.4 (\text{band } 4 / \text{band } 3) - 6785.3 (\text{band } 5 / \text{band } 4) + 16,967.5 (\text{band } 4 / \text{band } 2) + 55,042.3 (\text{band } 3 / \text{band } 2) - 3467.3 (\text{band } 4 / \text{band } 7) + 3401.3 (\text{band } 3 / \text{band } 1)$
Zn	$-43,904.42 + 21.2 \text{ OC} + 5.5 \text{ clay} + 141.9 \text{ Fe} + 45,456.4 (\text{band } 2 / \text{band } 3) + 25,272.8 (\text{band } 3 / \text{band } 2) + -31,119.0 (\text{band } 4 / \text{band } 7) + 176.609 (\text{band } 4)$

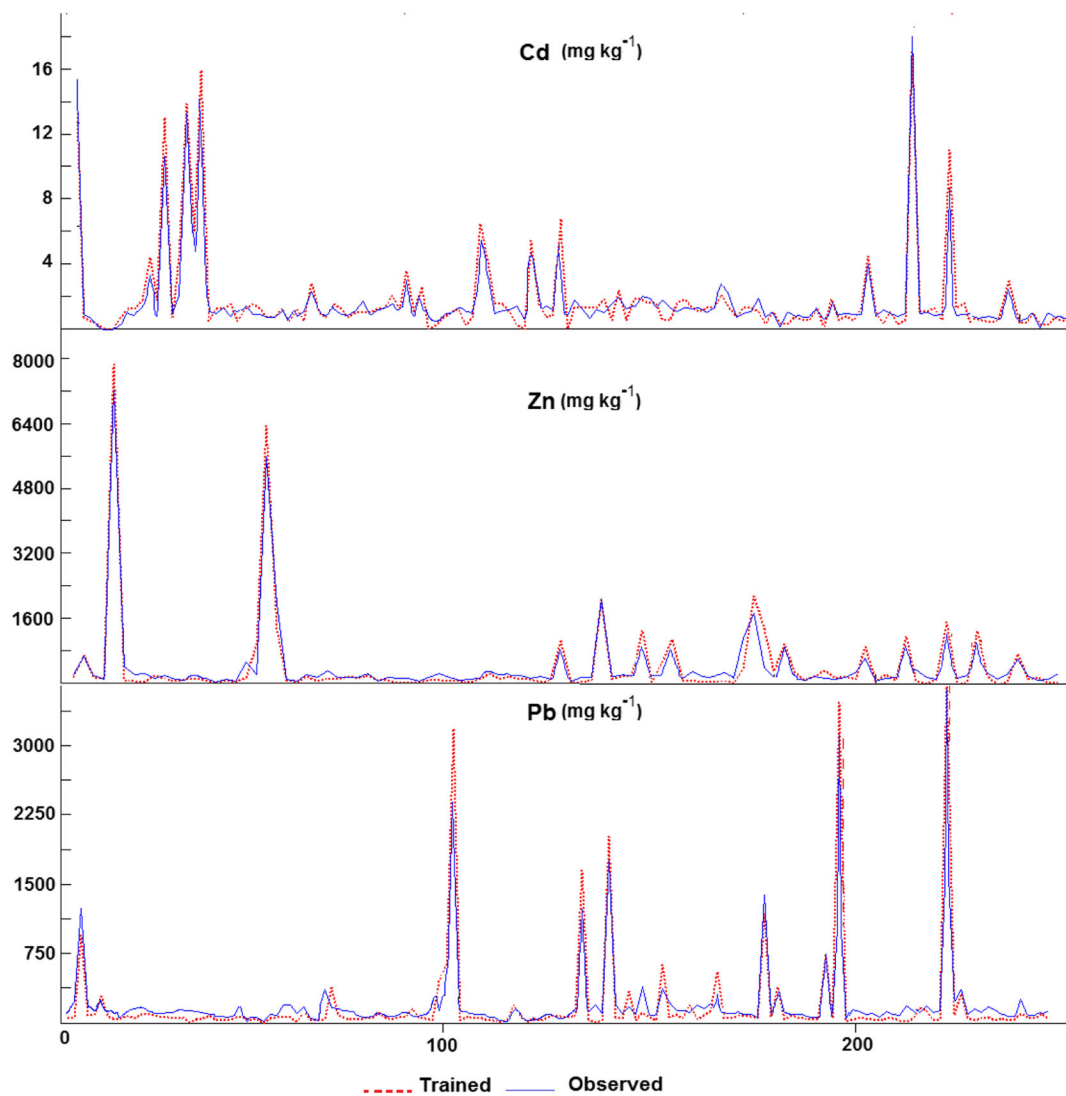


Fig. 3 Observed and training data of Cd, Pb and Zn with ANN-GA model

$$G_i^* = \frac{\sum_{j=1}^N w_{ij}(d)x_j}{\sum_{j=1}^n x_j} \tag{4}$$

G_i is the G^* index; N is the number of spatial observation; $w_{ij}(d)$ is the spatial weighting value within a specified distance d of a particular observation pixel i ; x_j standardized observed value of pixel j .

Soil sampling for the streams and roads

To evaluate the role of surface water and streams in soil heavy metal contamination and distribution, ArcHydro tool in ArcGIS was used to delineate stream network, based on the digital elevation map (DEM) of the study area. The stream maps were checked by field observation and a global position system (GPS) instrument. Forty-eight soil samples (0–5-cm depths) with intervals of 750 m were collected and analyzed for the heavy metal contents. A 100-m buffer zone was considered as a study section along the streams. Kriging interpolation method was employed to produce the gradient maps of heavy metal distribution along the streams. This method has been widely employed in many studies on heavy metal contaminations, especially on heavy metal distribution maps (Alam et al. 2015; Alyazichi et al. 2015; Moore et al. 2016; Qi et al. 2016). The exponential semivariance model (ordinary kriging) was applied for the spatial interpolation given the lower minimum RMSE and average standard error of cross-validation compared to the Gaussian and spherical models.

To study the impact of traffic on the soil heavy metal concentration, nine roadside areas were

investigated with an interval of 2 km along the roads: five areas from the Tabriz-Tehran freeway (line 1 in Fig. 1) and four areas from Basij Expressway (line 2 in Fig. 1). In each area, four samples were collected from roadsides at intervals of 10, 30, 60 and 100 m. The heavy metal concentrations were determined for each sample.

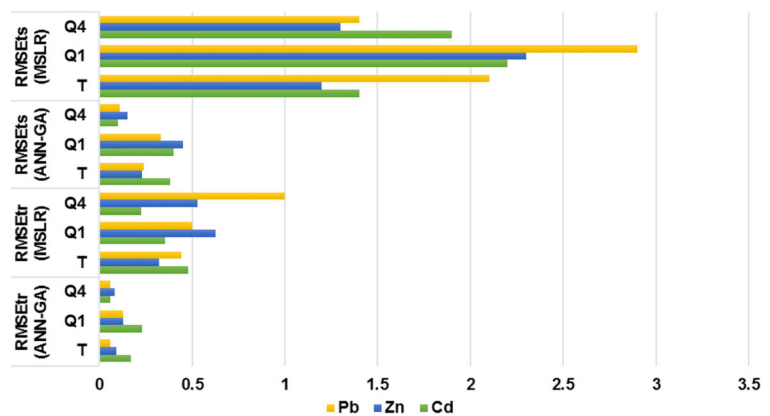
Results and discussion

Geochemical analysis

The statistical results of the measured soil properties and heavy metals are shown in Table 1. The means of organic carbon and Fe contents of the soil surface were 0.78 and 0.95%, respectively. The dominant soil textures were of the classes of sandy loam (SL) and sandy clay loam (SCL) with low clay contents (26.51%).

The average concentrations of Cd, Pb and Zn were 1.92, 354.98 and 501.10 mg kg⁻¹, respectively. The heavy metal concentrations of the samples varied for Cd (0.88–17.61 mg kg⁻¹), Pb (13.38–3475 mg kg⁻¹) and Zn (12.50–7253.6 mg kg⁻¹). In line with the suggested critical limits for heavy metals by the standards of the Department of Environment in Islamic Republic of Iran (Department of Environment, Islamic Republic of Iran 2013), the mean values of Pb (354.98 mg kg⁻¹) and Zn (501.10 mg kg⁻¹) were at a risk level as shown in Table 2. A Cd concentration was classified in the “no risk” level. Values of %RSD and %REC represented good accuracy and thus confirmed the reliability of the results.

Fig. 4 RMSE results of ANN-GA and MSLR models for Cd, Pb and Zn (RMSE root mean square error, t_r train data, t_s test data, t total data, $Q1$ quartile 1, $Q4$ quartile 4)



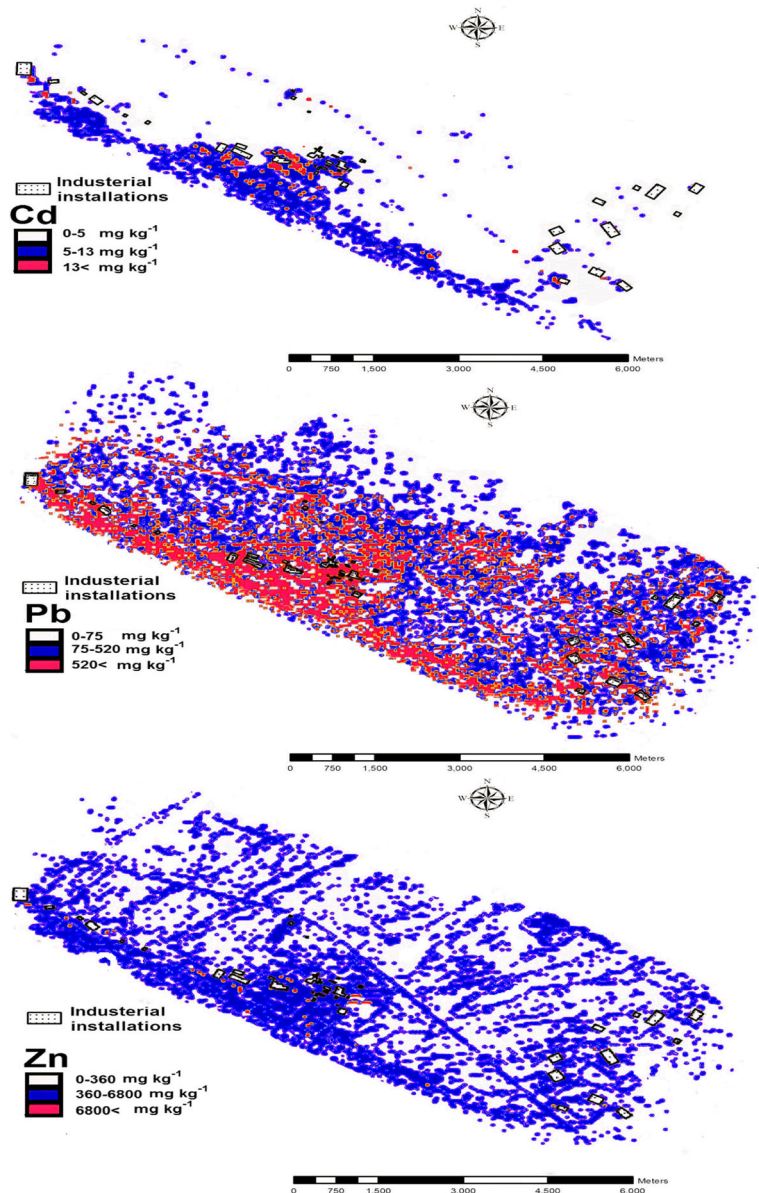
Modeling

The results of training ($n = 240$) and test ($n = 60$) models for MSLR and ANN-GA are shown in Table 3. The root mean square error of training data using ANN-GA for Cd, Pb and Zn were 0.85, 0.91 and 0.90, respectively, and were 0.41, 0.58 and 0.57, respectively, using MSLR. The root mean square error of test data using ANN-GA for Cd, Pb and Zn were 0.91, 0.86 and 0.76, respectively, and were 0.51, 0.56 and 0.63, respectively,

using MSLR. The training and test RMSE of ANN-GA model were less than the corresponding RMSE of MSLR model, and R^2 of ANN-GA model were higher than the corresponding R^2 of MSLR model (Table 3). The model errors of ANN-GA were lower than MSLR.

The salient features of these models include usage of various band ratios which can present the larger coefficient of determination (R^2) in linear models. Visible bands (1, 2, and 3) alongside infrared band (4) in the obtained relations are among effective variables which

Fig. 5 Maps predicting heavy metal (mg kg^{-1}) distribution in studied area (no risk area (white), risk area (blue), high risk area (red), for heavy metal concentration)



have been used in all of the equations. These bands alongside their ratios have been considered suitable for predicting the concentration of heavy metals by various researchers (Bien et al. 2005; Wu et al. 2007; Wang et al.

2014). Band 7 and the ratios associated with it including 4 to 7 band ratio and 5 to 7 band ratio were in the band formulation obtained with heavy metals (Table 4). Choe et al. (2008) examined the characteristics of spectral

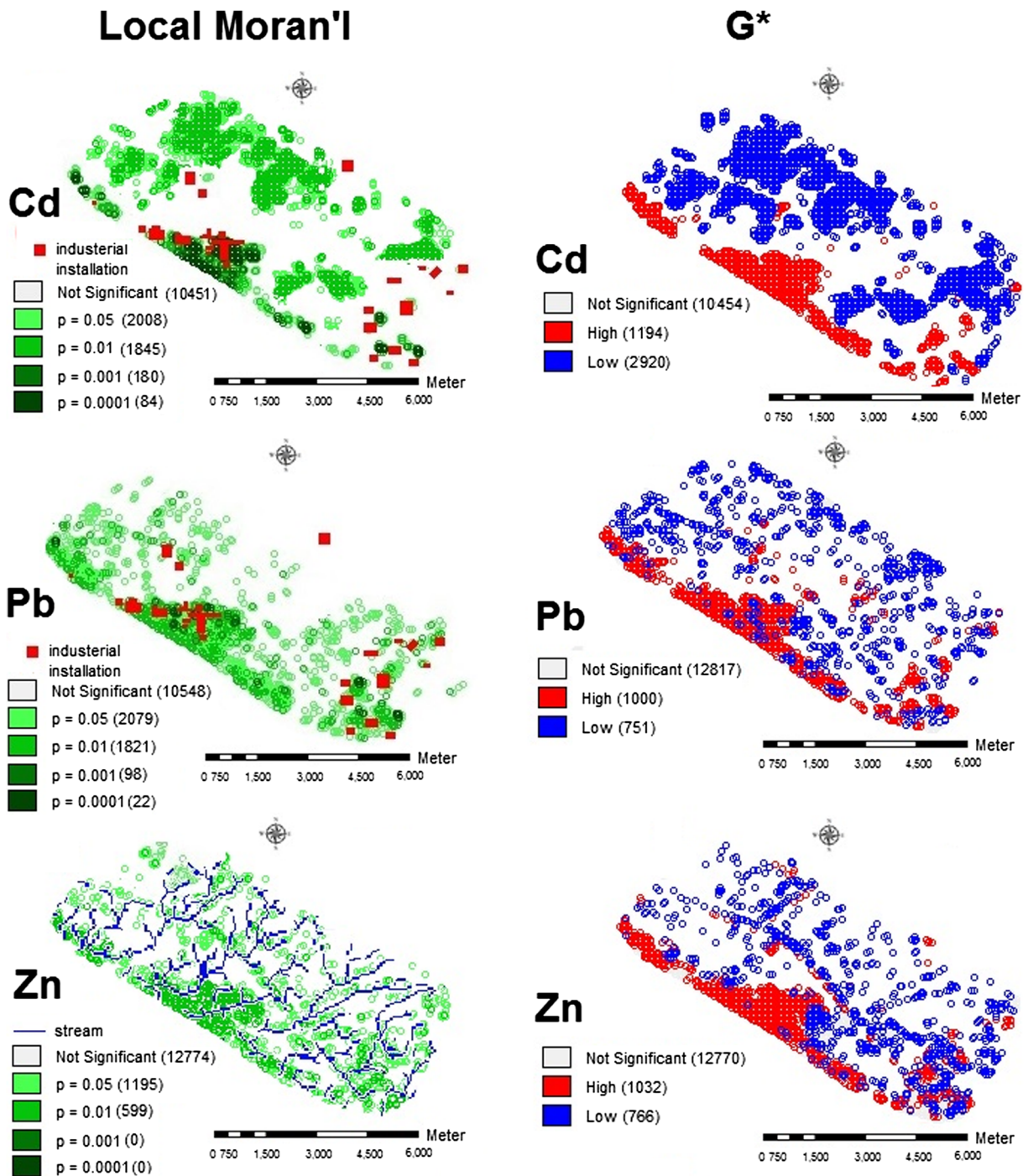


Fig. 6 Spatial autocorrelation of heavy metal distribution using local Moran index and Getis-Ord Gi* (significant levels vs. number of related pixels in bracket)

absorption of heavy metals including arsenic, lead, and zinc in laboratory. They introduced region 2200 nm (a close infrared spectral range, the range of band 7) as a desirable absorption region for these metals.

The training process of ANN-GA is presented in Fig. 3, showing a good match between predicted and observed data, especially in high concentrations.

In more detailed exploration, RMSE of quartile 1 (Q1) and 4 (Q4) showed that in most cases, error of Q1 (low concentrations) was higher than error of Q4 (high concentrations) (Fig. 4). It showed the good ability of ANN-GA linear models for estimating higher concentration of heavy metals in comparison to linear models. Choe et al. (2008) also reported weak ability of linear model in estimation of high concentration of heavy metals by remote sensing technique.

In line with our results, Tsoukalas and Fragiadakis (2016) reported that the prediction of risk assessment using GA is more useful and efficient compared to when a multivariate regression analysis is utilized. Zhou et al. (2015) applied statistical analysis, ANN, and ANN-GA to predict As, Cd, Cr, Cu, Hg, Ni, Pb and Zn and found similar results. They reported that ANN-GA performance in source mapping and point finding is more accurate when using high concentrations of heavy metals.

Heavy metal distribution map

The best accuracy for heavy metal distributions was obtained using ANN-GA; thus, distribution maps were prepared based on this method. The heavy metal distribution maps for Cd, Pb and Zn provided

using ANN-GA model are shown in Fig. 5. The maps displayed heavy metal concentration in three classes as shown in Table 2: no risk, risk and high risk classes. Based on the maps, high Cd values were mainly found around industrial zones and southern parts of the study area. Approximately, the similar spatial patterns in the risk and high risk classes can be observed for Pb and Zn around industrial installations.

Critical concentration areas of heavy metals were detected using maps for each pollution classes. Areas of 2155 ha of the studied area were categorized into the risk class for lead, 50 ha for cadmium and 9 ha for zinc. Local Moran's index and Getis-Ord G_i^* were conducted to evaluate and compare the spatial autocorrelation of heavy metals and draw the spatial patterns of their differences (Fig. 6).

Significant clusters of Cd (Fig. 6, 28.3% of total area) were located in the southern part of the study area (5), while the highest autocorrelation ($p < 0.01$) of Cd (14.5%) was found around the industrial zone with a clumped pattern. Of the study area, 4.1% was classified into high risk of Zn pollution, while 13.3% had high risk of Pb contamination. The significance of Pb clusters ($p < 0.05$) increased from east to west in direction of the prevailing wind. Wind force could move fine particles from their sources and spread them to the surrounding areas and could affect the distribution of heavy metals (Chen et al. 2012; Connan et al. 2013). In line with the results of Dore et al. (2014), Pb had the highest wet and dry deposition.

The clusters of heavy metal concentration as calculated by Getis-Ord G_i^* statistics are shown in Fig. 6.

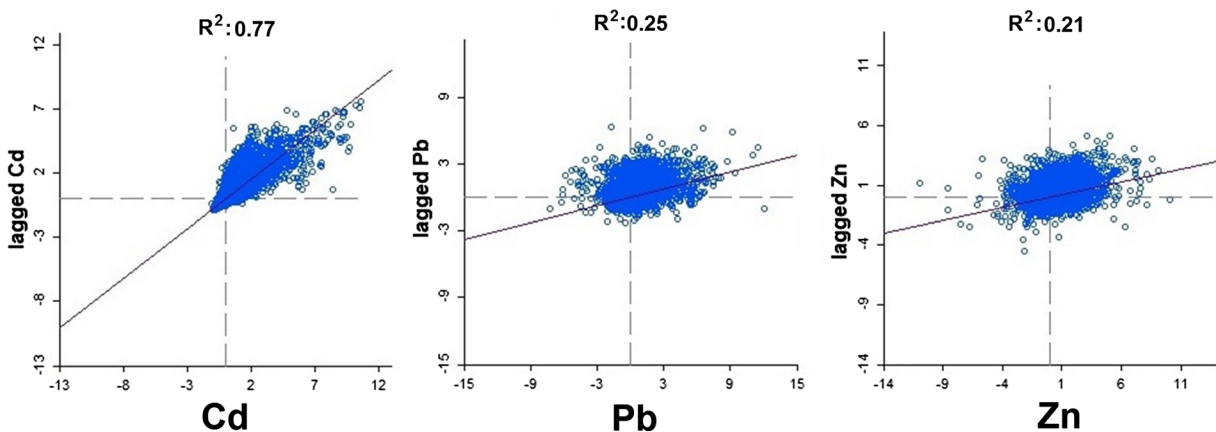


Fig. 7 Moran scatter plot for Cd, Pb and Zn

High values of Cd (8.2% of total data) were noted around the industrial installations, while low values (20.0%) were in farther distances. The source of high concentration for Cd would probably differ from low concentration, given that there was a gap (not significant) between these two classes and the gradual change from low to high concentration was not noted. The concentration of Zn and Pb showed similar pattern (Fig. 6). The scatter plot of Moran index for Cd showed that Cd values were more of a cross 1:1 line (0.77) showing more positive correlation (Fig. 7). Higher Moran index of Cd than Pb (0.25) and Zn (0.21) confirmed the high positive spatial aggregation of Cd.

The impact of main factors on heavy metal distribution

Heavy metal distribution could be affected by different sources in the study area such as industrial installations, roads, highway, and agricultural activities. Therefore, in the following sections, the main factors that could affect the contamination of heavy metals were described.

Streams

The study of five tributaries of streams (Fig. 8) showed that the concentration of Cd (Fig. 8b), Pb (Fig. 8c) and Zn (Fig. 8d) increased toward

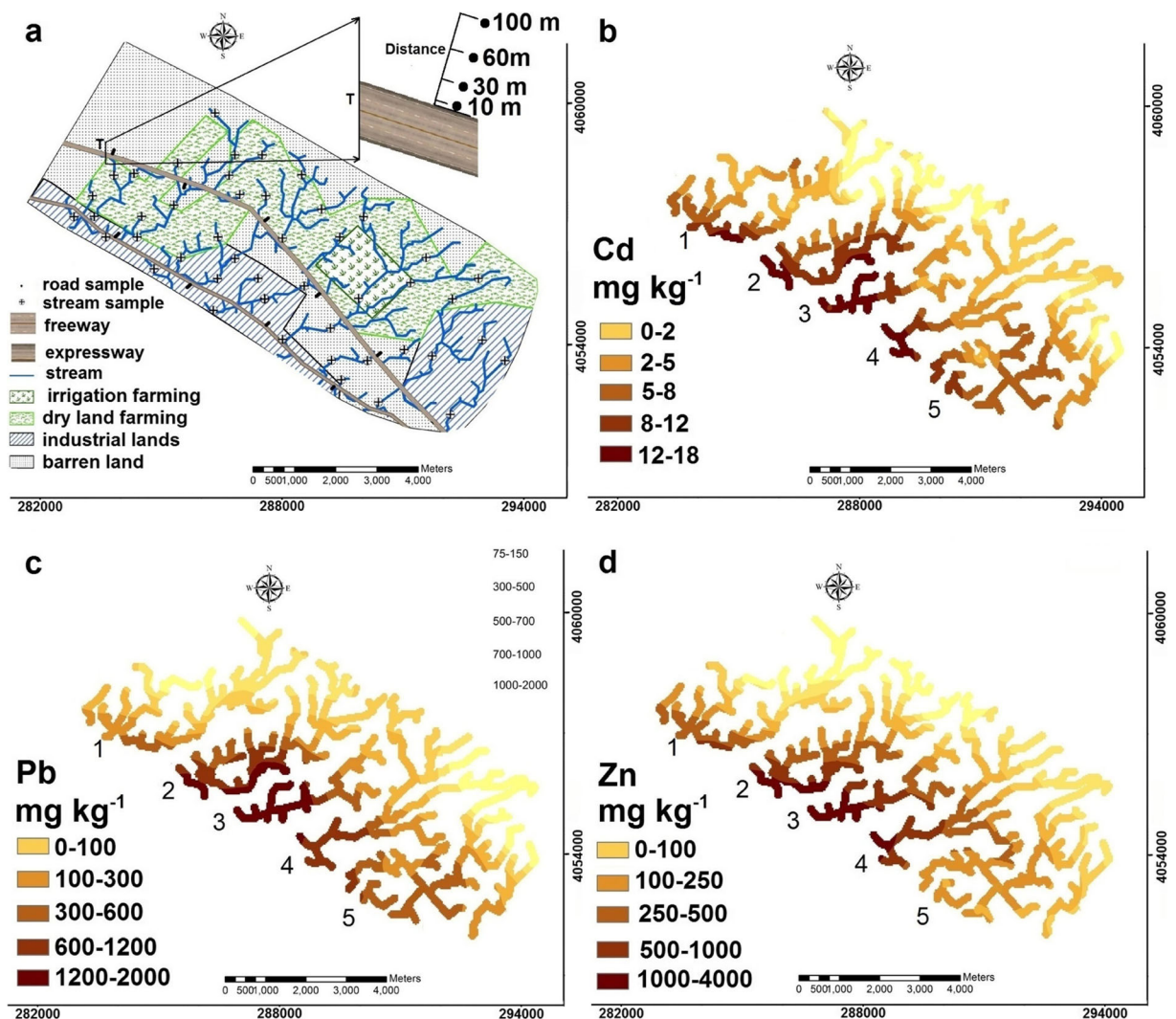


Fig. 8 a Location map and land use, stream and sampling points along the studied main stream, and roads. Spatial distribution maps of heavy metal concentration in streams and showing the five sections for **b** Cd, **c** Pb and **d** Zn

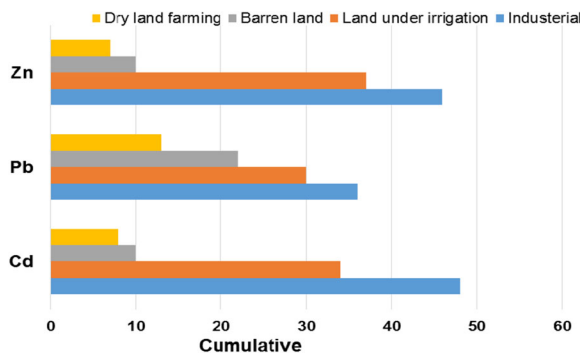


Fig. 9 Cumulative percentages of heavy metal concentration under different land uses

downstream. The concentrations of Cd, Pb and Zn in downstream of stretch 3 are in 12–8, 1200–200, and 1000 mg kg⁻¹ ranges and seem to have the highest accumulation. This stretch passed through the industrial land use, where the soil surface colloids alongside heavy metals were washed and transferred to the streams from the adjacent land use, thus leading to a rise in the heavy metal loading rates in the stretch. The colloids, including clay and organic matter, were strongly pH-dependent with a negative charge in alkaline pH of the study area (Table 1). The heavy metals were bounded to the negatively charged carboxyl and hydroxyl agent groups. Therefore, they could be transported by soil erosion (Dube et al. 2001).

Similar to the study of Schaidler et al. (2014), the results of the present research demonstrated that additional accumulation of the heavy metals in downstreams was caused by runoff. They studied the temporal changes of Cd, Pb, and Zn in the mining-impacted streams and reported that Zn, Pb, and Cd annual accumulations were 8800, 160, and

15 kg year⁻¹, respectively. As a replicate to an earlier study conducted by Cope et al. (2008), the substantial loadings of these elements in the streams were found to occur in the same area as the drainage points of the industrial areas.

Land use

The cumulative percentages of heavy metal concentration under different land uses are summarized in Fig. 9. Four land uses, including industrial zones, barren land, irrigation farming, and dryland farming, are recognized in the studied area (Fig. 8a). The concentration of Cd, Pb, and Zn under different land uses was in the following order: industrial lands > irrigation farming > barren land > dryland farming (Fig. 9).

High heavy metal levels in industrial lands were noted as a result of residual deposits, produced from heavy metal purification process. High content of heavy metals under irrigation could be attributed to the excessive use of chemical fertilizer (Hani and Pazira 2011). Phosphate rocks naturally contain high Cd levels (Jiao et al. 2012), and the application of phosphate fertilizers could increase Cd content in agricultural soil (Cai et al. 2012). The use of chemical fertilizer has significant effect on Pb (Atafar et al. 2010) and Zn (Sun et al. 2013) concentration. In spite of chemical fertilization of dryland farming, the closer distance to industrial zones led to higher contamination of barren lands when compared to the dryland farming.

Roads

The impact of distance from main roads on soil contamination of heavy metals is shown in Fig. 10a, b. To study

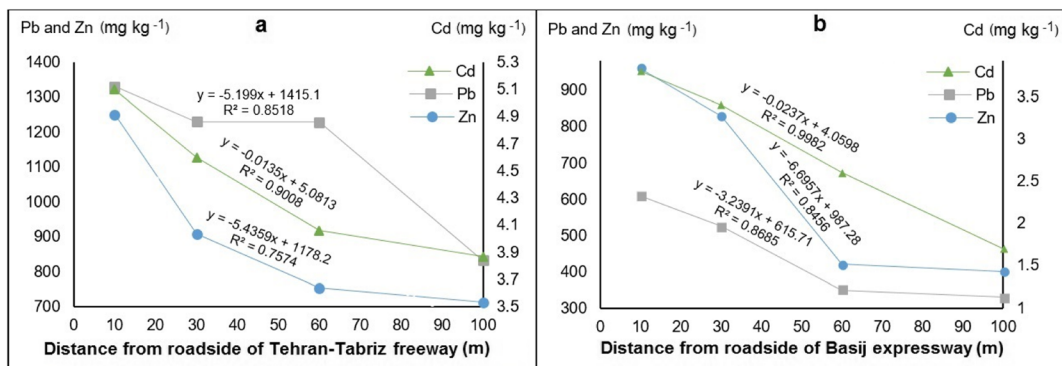


Fig. 10 Heavy metal distribution patterns in roadsides. **a** Tehran-Tabriz freeway. **b** Basij Expressway

the effect of traffic on heavy metal distribution, several researchers have measured heavy metal concentration at different distances from roadsides (Chen et al. 2010; Yan et al. 2013a,b; Wiseman et al. 2013; Werkenthin et al. 2014). Cd, Pb, and Zn decreased from 5.1, 1130, and 1251 mg kg⁻¹ to 3.8, 832, and 712 mg kg⁻¹, respectively, by increasing distance from the Tabriz-Tehran freeway (Fig. 10a).

The results further illustrated that Cd, Pb and Zn decreased from 3.8, 610, and 960 mg kg⁻¹ to 1.7, 330, and 400 mg kg⁻¹, respectively, in the roadside of Basij Expressway (Fig. 10b). Despite the fact that the concentration of soil heavy metals is reduced by restricting distance from roads to 100 m, the amount of elements was still high and in a dangerous level for agricultural productions. Fuel combustion and gases emitted from vehicles are the main source of air pollution (more than 50 µg m⁻³) along with soil heavy metal contamination around the roads (Farahmandkia et al. 2011). This study indicated that crop production and agriculture activities must be restricted to a distance of 60 m from main roads.

Conclusion

High concentrations of Cd, Pb and Zn were observed in the study area indicating that industrial activities had effect on heavy metal distributions. Sampling around the roads and streams showed that traffic was one of the major sources of heavy metal pollution, which were washed off into the streams, rivers, and downstream lands. The efficiency of ANN-GA and MSLR was assessed in the prediction of soil heavy metal distribution in different land uses based on remote sensing data (ETM+). The results confirmed the higher ability of ANN-GA for predicting heavy metal distribution, particularly in high concentration of elements when compared to MSLR. The local Moran's index was found as a useful complementary analysis in the remote sensing technique, which provided the regional hotspots of heavy metal distributions, and was thus useful in the source identification of heavy metals. The pixel sizes of satellite images had a significant role in the accuracy of the remote sensing models. Using images with smaller pixel sizes and higher special resolutions could result in more accurate outcomes to be recommended for future research. This study indicated that the combination of AAN-GA, remote sensing technique, and

clustering analysis can be considered as a quick and low-cost method. This approach can be used for providing reliable information regarding the spatial distribution of soil heavy metals and their pollutant sources.

References

- Alam, N., Ahmad, S. R., Qadir, A., Ashraf, M. I., Lakhan, C., & Lakhan, V. C. (2015). Use of statistical and GIS techniques to assess and predict concentrations of heavy metals in soils of Lahore City, Pakistan. *Environmental Monitoring and Assessment*, 187(10), 1–11. doi:10.1007/s10661-015-4855-1.
- Alyazichi, Y. M., Jones, B. G., & McLean, E. (2015). Source identification and assessment of sediment contamination of trace metals in Kogarah Bay, NSW, Australia. *Environmental Monitoring and Assessment*, 187(2), 1–10. doi:10.1007/s10661-014-4238-z.
- Anselin, L. (1995). Local indicators of spatial association—LISA. *Geographical Analysis*, 27(2), 93–115.
- Asami, T. (1984). Pollution of soils by cadmium. In *Changing metal cycles and human health* (pp. 95–111). New York: Springer Berlin Heidelberg.
- Askari, M. S., O'Rourke, S. M., & Holden, N. M. (2015). Evaluation of soil quality for agricultural production using visible–near-infrared spectroscopy. *Geoderma*, 243–244, 80–91. doi:10.1016/j.geoderma.2014.12.012.
- Asmaryan, S. G., Muradyan, V., Sahakyan, L., Saghatlyan, A., & Warner, T. (2014). Development of remote sensing methods for assessing and mapping soil pollution with heavy metals. *Global Soil Map: Basis of the global spatial soil information system*, 429.
- Atafar, Z., Mesdaghinia, A., Nouri, J., Homae, M., Yunesian, M., Ahmadimoghaddam, M., et al. (2010). Effect of fertilizer application on soil heavy metal concentration. *Environmental Monitoring and Assessment*, 160(1–4), 83–89. doi:10.1007/s10661-008-0659-x.
- Bien, J. D., ter Meer, J., Rulkens, W. H., & Rijnaarts, H. H. M. (2005). A GIS-based approach for the long-term prediction of human health risks at contaminated sites. *Environmental Monitoring and Assessment*, 9(4), 221–226. doi:10.1007/s10666-005-0909-z.
- Boszke, L., & Astel, A. (2009). Application of neural-based modeling in an assessment of pollution with mercury in the middle part of the Warta River. *Environmental Monitoring and Assessment*, 152(1), 133–147. doi:10.1007/s10661-008-0302-x.
- Cai, L., Xu, Z., Ren, M., Guo, Q., Hu, X., Hu, G., et al. (2012). Source identification of eight hazardous heavy metals in agricultural soils of Huizhou, Guangdong Province, China. *Ecotoxicology and Environmental Safety*, 78, 2–8. doi:10.1016/j.ecoenv.2011.07.004.
- Chang, C. L., Lo, S. L., & Yu, S. L. (2006). The parameter optimization in the inverse distance method by genetic algorithm for estimating precipitation. *Environmental Monitoring and Assessment*, 117(1), 145–155. doi:10.1007/s10661-006-8498-0.

- Chen, X., Xia, X., Zhao, Y., & Zhang, P. (2010). Heavy metal concentrations in roadside soils and correlation with urban traffic in Beijing, China. *Journal of Hazardous Materials*, *181*(1–3), 640–646. doi:10.1016/j.jhazmat.2010.05.060.
- Chen, Y., Liu, Y., Liu, Y., Lin, A., Kong, X., Liu, D., et al. (2012). Mapping of Cu and Pb contaminations in soil using combined geochemistry, topography, and remote sensing: a case study in the Le'an River floodplain, China. *International Journal of Environmental Research and Public Health*, *9*(5), 1874–1886. doi:10.3390/ijerph9051874.
- Choe, E., van der Meer, F., van Ruitenbeek, F., van der Werff, H., de Smeth, B., & Kim, K. W. (2008). Mapping of heavy metal pollution in stream sediments using combined geochemistry, field spectroscopy, and hyperspectral remote sensing: a case study of the Rodalquilar mining area, SE Spain. *Remote Sensing of Environment*, *112*(7), 3222–3233. doi:10.1016/j.rse.2008.03.017.
- Connan, O., Maro, D., Hébert, D., Rounsard, P., Goujon, R., Letellier, B., et al. (2013). Wet and dry deposition of particles associated metals (Cd, Pb, Zn, Ni, Hg) in a rural wetland site, Marais Vernier, France. *Atmospheric Environment*, *67*, 394–403. doi:10.1016/j.atmosenv.2012.11.029.
- Cook, N. J., Ciobanu, C. L., Pring, A., Skinner, W., Shimizu, M., Danyushevsky, L., et al. (2009). Trace and minor elements in sphalerite: a LA-ICPMS study. *Geochimica et Cosmochimica Acta*, *73*(16), 4761–4791. doi:10.1016/j.gca.2009.05.045.
- Cope, C. C., Becker, M. F., Andrews, W. J., & DeHay, K. (2008). Streamflow, water quality, and metal loads from chat leachate and mine outflow into Tar Creek, Ottawa County, Oklahoma, U. S. Geological Survey, Scientific Investigations Report 2007–5115.
- Department of Environment, Islamic Republic of Iran. (2013). Soil resources quality standards and its directions. 162 pp.
- Dore, A. J., Hallsworth, S., McDonald, A. G., Werner, M., Kryza, M., Abbot, J., et al. (2014). Quantifying missing annual emission sources of heavy metals in the United Kingdom with an atmospheric transport model. *Science of the Total Environment*, *479–480*(0), 171–180. doi:10.1016/j.scitotenv.2014.02.001.
- Dube, A., Zbytniewski, R., Kowalkowski, T., Cukrowska, E., & Buszewski, B. (2001). Adsorption and migration of heavy metals in soil. *Polish Journal of Environmental Studies*, *10*(1), 1–10.
- Farahmandkia, Z., Mehrasbi, M., & Sekhavatjou, M. (2011). Relationship between concentrations of heavy metals in wet precipitation and atmospheric PM10 particles in Zanjan. *Iranian Journal of Environmental Health Science & Engineering*, *8*(1), 49–56.
- Fu, W., Zhao, K., Zhang, C., & Tunney, H. (2011). Using Moran's I and geostatistics to identify spatial patterns of soil nutrients in two different long-term phosphorus application plots. *Journal of Plant Nutrition and Soil Science*, *174*(5), 785–798. doi:10.1002/jpln.201000422.
- Fu, F., & Wang, Q. (2011). Removal of heavy metal ions from wastewaters: a review. *Journal of Environmental Management*, *92*(3), 407–418. doi:10.1016/j.jenvman.2010.11.011.
- Gannouni, S., Rebai, N., & Abdeljaoued, S. (2012). A spectroscopic approach to assess heavy metals contents of the mine waste of Jalta and Bougrine in the north of Tunisia. *Journal of Geographic Information System*, *4*(3), 242–253. doi:10.4236/jgis.2012.43029.
- Gee, G. W., Bauder, J. W., & Klute, A. (1986). Particle-size analysis. *Methods of soil analysis. Part 1. Physical and mineralogical methods*, 383–411.
- Getis, A., & Ord, J. K. (1992). The analysis of spatial association by use of distance statistics. *Geographical Analysis*, *24*(3), 189–206. doi:10.1111/j.1538-4632.1992.tb00261.x.
- Gill, S. S., & Tuteja, N. (2011). Cadmium stress tolerance in crop plants: probing the role of sulfur. *Plant Signaling & Behavior*, *6*(2), 215–222. doi:10.4161/psb.6.2.14880.
- Guala, S. D., Vega, F. A., & Covelo, E. F. (2010). The dynamics of heavy metals in plant–soil interactions. *Ecological Modelling*, *221*(8), 1148–1152. doi:10.1016/j.ecolmodel.2010.01.003.
- Hani, A., & Pazira, E. (2011). Heavy metals assessment and identification of their sources in agricultural soils of Southern Tehran, Iran. *Environmental Monitoring and Assessment*, *176*(1–4), 677–691. doi:10.1007/s10661-010-1612-3.
- Hong-Yan, R. E. N., Zhuang, D. F., Singh, A. N., Jian-Jun, P. A. N., Dong-Sheng, Q. I. U., & Run-He, S. H. I. (2009). Estimation of As and Cu contamination in agricultural soils around a mining area by reflectance spectroscopy: a case study. *Pedosphere*, *19*(6), 719–726. doi:10.1016/S1002-0160(09) 60167-3.
- Icaga, Y. (2005). Genetic algorithm usage in water quality monitoring networks optimization in Gediz (Turkey) river basin. *Environmental Monitoring and Assessment*, *108*(1), 261–277. doi:10.1007/s10661-005-4328-z.
- Ishioka, F., Kurihara, K., Suito, H., Horikawa, Y., & Ono, Y. (2007). Detection of hotspots for three-dimensional spatial data and its application to environmental pollution data. *Journal of Environmental Science for Sustainable Society*, *1*, 15–24. doi:10.3107/jesss.1.15.
- Jarmer, T., Vohland, M., Lilienthal, H., & Schnug, E. (2008). Estimation of some chemical properties of an agricultural soil by spectroradiometric measurements. *Pedosphere*, *18*(2), 163–170. doi:10.1016/S1002-0160(08)60004-1.
- Jiao, W., Chen, W., Chang, A. C., & Page, A. L. (2012). Environmental risks of trace elements associated with long term phosphate fertilizers applications: a review. *Environmental Pollution*, *168*(0), 44–53. doi:10.1016/j.envpol.2012.03.052.
- Kabata-Pendias, A. (2010). *Trace elements in soils and plants*. USA: CRC press.
- Kaiser, M., Aboulela, H., El Serehy, H., & Ezz Edin, H. (2010). Spectral enhancement of SPOT imagery data to assess marine pollution near Port Said, Egypt. *International Journal of Remote Sensing*, *31*(7), 1753–1764. doi:10.1080/01431160902926624.
- Kemper, T., & Sommer, S. (2002). Estimate of heavy metal contamination in soils after a mining accident using reflectance spectroscopy. *Environmental Science & Technology*, *36*(12), 2742–2747. doi:10.1021/es015747j.
- Lasaponara, R., Leucci, G., Masini, N., Persico, R., & Scardozzi, G. (2016). Towards an operative use of remote sensing for exploring the past using satellite data: the case study of Hierapolis (Turkey). *Remote Sensing of Environment*, *174*, 148–164. doi:10.1016/j.rse.2015.12.016.

- Liu, D., Wang, Z., Zhang, B., Song, K., Li, X., Li, J., et al. (2006a). Spatial distribution of soil organic carbon and analysis of related factors in croplands of the black soil region, Northeast China. *Agriculture, Ecosystems & Environment*, 113(1–4), 73–81. doi:10.1016/j.agee.2005.09.006.
- Liu, X., Wu, J., & Xu, J. (2006b). Characterizing the risk assessment of heavy metals and sampling uncertainty analysis in paddy field by geostatistics and GIS. *Environmental Pollution*, 141(2), 257–264. doi:10.1016/j.envpol.2005.08.048.
- Liu, Y., Lv, J., Zhang, B., & Bi, J. (2013). Spatial multiscale variability of soil nutrients in relation to environmental factors in a typical agricultural region, Eastern China. *Science of the Total Environment*, 450–451, 108–119. doi:10.1016/j.scitotenv.2013.01.083.
- Mance, G., & Worsfold, P. (1988). *Pollution threat of heavy metals in aquatic environments*. London: Elsevier 372 pp.
- Mehra, O., & Jackson, M. (1958). Iron oxide removal from soils and clays by a dithionite-citrate system buffered with sodium bicarbonate. In: National conference on clays and clays minerals, 7: 317–327.
- Meindl, G. A., Bain, D. J., & Ashman, T. L. (2014). Nickel accumulation in leaves, floral organs and rewards varies by serpentine soil affinity. *AoB Plants*, 6(plu036). doi:10.1093/aobpla/plu036.
- Miao, Q., Liu, R., Wang, Y., Song, J., Quan, Y., & Li, Y. (2015). Remote sensing image fusion based on shearlet and genetic algorithm. In *Bio-Inspired Computing-Theories and Applications* (pp. 283–294). New York: Springer Berlin Heidelberg.
- Moore, F., Sheykhi, V., Salari, M., & Bagheri, A. (2016). Soil quality assessment using GIS-based chemometric approach and pollution indices: Nakhak mining district, Central Iran. *Environmental Monitoring and Assessment*, 188(4), 1–16. doi:10.1007/s10661-016-5152-3.
- Moros, J., de Vallejuelo, S. F. O., Gredilla, A., de Diego, A., Madariaga, J. M., Garrigues, S., et al. (2009). Use of reflectance infrared spectroscopy for monitoring the metal content of the estuarine sediments of the Nerbioi-Ibaizabal River (Metropolitan Bilbao, Bay of Biscay, Basque Country). *Environmental Science & Technology*, 43(24), 9314–9320. doi:10.1021/es9005898.
- Overmars, K. P., de Koning, G. H. J., & Veldkamp, A. (2003). Spatial autocorrelation in multi-scale land use models. *Ecological Modelling*, 164(2–3), 257–270. doi:10.1016/S0304-3800(03)00070-X.
- Pourjabbar, A., Sárbu, C., Kostarelos, K., Einax, J. W., & Büchel, G. (2014). Fuzzy hierarchical cross-clustering of data from a abandoned mine site contaminated with heavy metals. *Computers & Geosciences*, 72(0), 122–133. doi:10.1016/j.cageo.2014.07.004.
- Qi, J., Zhang, H., Li, X., & Zhang, G. (2016). Concentrations, spatial distribution, and risk assessment of soil heavy metals in a Zn-Pb mine district in southern China. *Environmental Monitoring and Assessment*, 188(7), 1–11. doi:10.1007/s10661-016-5406-0.
- Schaider, L. A., Senn, D. B., Estes, E. R., Brabander, D. J., & Shine, J. P. (2014). Sources and fates of heavy metals in a mining impacted stream: temporal variability and the role of iron oxides. *Science of the Total Environment*, 490, 456–466. doi:10.1016/j.scitotenv.2014.04.126.
- Şenkal, O. (2010). Modeling of solar radiation using remote sensing and artificial neural network in Turkey. *Energy*, 35(12), 4795–4801. doi:10.1016/j.energy.2010.09.009.
- Shahbazi, Y., Ahmadi, F., & Fakhari, F. (2016). Voltammetric determination of Pb, Cd, Zn, Cu and Se in milk and dairy products collected from Iran: an emphasis on permissible limits and risk assessment of exposure to heavy metals. *Food Chemistry*, 192, 1060–1067. doi:10.1016/j.foodchem.2015.07.123.
- Shi, T., Chen, Y., Liu, Y., & Wu, G. (2014). Visible and near infrared reflectance spectroscopy—an alternative for monitoring soil contamination by heavy metals. *Journal of Hazardous Materials*, 265, 166–176. doi:10.1016/j.jhazmat.2013.11.059.
- Slonecker, T., Fisher, G. B., Aiello, D. P., & Haack, B. (2010). Visible and infrared remote imaging of hazardous waste: a review. *Remote Sensing*, 2(11), 2474–2508. doi:10.3390/rs2112474.
- Song, L., Jian, J., Tan, D. J., Xie, H. B., Luo, Z. F., & Gao, B. (2015). Estimate of heavy metals in soil and streams using combined geochemistry and field spectroscopy in Wansheng mining area, Chongqing, China. *International Journal of Applied Earth Observation and Geoinformation*, 34, 1–9. doi:10.1016/j.jag.2014.06.013.
- Sun, C., Liu, J., Wang, Y., Sun, L., & Yu, H. (2013). Multivariate and geostatistical analyses of the spatial distribution and sources of heavy metals in agricultural soil in Dehui, Northeast China. *Chemosphere*, 92(5), 517–523. doi:10.1016/j.chemosphere.2013.02.063.
- Templ, M., Filzmoser, P., & Reimann, C. (2008). Cluster analysis applied to regional geochemical data: problems and possibilities. *Applied Geochemistry*, 23(8), 2198–2213. doi:10.1016/j.apgeochem.2008.03.004.
- Thenkabail, P. S., Lyon, J. G., & Huete, A. (2011). *Hyperspectral remote sensing of vegetation*. New York: CRC Press.
- Tsoukalas, V., & Fragiadakis, N. (2016). Prediction of occupational risk in the shipbuilding industry using multivariable linear regression and genetic algorithm analysis. *Safety Science*, 83, 12–22. doi:10.1016/j.ssci.2015.11.010.
- Walky, A., & Black, I. (1934). An examination of the Degtiareff method for deterring soil organic matter and proposed modification of the chromic acid titration method. *Soil Science*, 63, 29–38.
- Wang, H., Dong, Y., Yang, Y., Toor, G. S., & Zhang, X. (2013). Changes in heavy metal contents in animal feeds and manures in an intensive animal production region of China. *Journal of Environmental Sciences*, 25(12), 2435–2442. doi:10.1016/S1001-0742(13)60473-8.
- Wang, J., Cui, L., Gao, W., Shi, T., Chen, Y., & Gao, Y. (2014). Prediction of low heavy metal concentrations in agricultural soils using visible and near infrared reflectance spectroscopy. *Geoderma*, 216(0), 1–9. doi:10.1016/j.geoderma.2013.10.024.
- Werkenthin, M., Kluge, B., & Wessolek, G. (2014). Metals in European roadside soils and soil solution—a review. *Environmental Pollution*, 189, 98–110. doi:10.1016/j.envpol.2014.02.025.
- Wiseman, C. L., Zereini, F., & Puttmann, W. (2013). Traffic related trace element fate and uptake by plants cultivated in roadside soils in Toronto, Canada. *Science of the Total Environment*, 442, 86–95. doi:10.1016/j.scitotenv.2012.10.051.

- Wu, L., Wang, Y., Long, J., & Liu, Z. (2015). An unsupervised change detection approach for remote sensing image using principal component analysis and genetic algorithm. In *Image and graphics* (pp. 589–602). New York City: Springer International Publishing.
- Wu, Y., Chen, J., Ji, J., Gong, P., Liao, Q., Tian, Q., et al. (2007). A mechanism study of reflectance spectroscopy for investigating heavy metals in soils. *Soil Science Society of America Journal*, 71(3), 918–926. doi:10.2136/sssaj2006.0285.
- Xia, X., Chen, J., Ma, H., & Ji, J. (2006). Assessment of cadmium contamination in the sediments of Changjiang (Yangtze) River by reflectance spectroscopy. *Chinese Journal of Geochemistry*, 25(1), 226–226. doi:10.1007/bf02840182.
- Xiao, Z., Liang, S., Wang, J., Chen, P., Yin, X., Zhang, L., et al. (2014). Use of general regression neural networks for generating the GLASS leaf area index product from time-series MODIS surface reflectance. *Geoscience and Remote Sensing, IEEE Transactions on*, 52(1), 209–223. doi:10.1109/TGRS.2013.2237780.
- Yan, X., Gao, D., Zhang, F., Zeng, C., Xiang, W., & Zhang, M. (2013a). Relationships between heavy metal concentrations in roadside topsoil and distance to road edge based on field observations in the Qinghai-Tibet Plateau, China. *International Journal of Environmental Research and Public Health*, 10(3), 762–775. doi:10.3390/ijerph10030762.
- Yan, X., Zhang, F., Gao, D., Zeng, C., Xiang, W., & Zhang, M. (2013b). Accumulations of heavy metals in roadside soils close to zhaling, eling and nam co lakes in the Tibetan plateau. *International Journal of Environmental Research and Public Health*, 10(6), 2384–2400. doi:10.3390/ijerph10062384.
- Zhang, C., Fay, D., McGrath, D., Grennan, E., & Carton, O. T. (2008). Statistical analyses of geochemical variables in soils of Ireland. *Geoderma*, 146(1–2), 378–390. doi:10.1016/j.geoderma.2008.06.013.
- Zhou, P., Zhao, Y., Zhao, Z., & Chai, T. (2015). Source mapping and determining of soil contamination by heavy metals using statistical analysis, artificial neural network, and adaptive genetic algorithm. *Journal of Environmental Chemical Engineering*, 3(4), 2569–2579. doi:10.1016/j.jece.2015.08.003.
- Zimdahl, R. L., & Skogerboe, R. K. (1977). Behavior of lead in soil. *Environmental Science & Technology*, 11(13), 1202–1207.